

Parameterization of Star-Shaped Volumes Using Green’s Functions

Jiazhi Xia^a, Ying He^a, Shuchu Han^a, Chi-Wing Fu^a, Feng Luo^b, and Xianfeng Gu^c

^aSchool of Computer Engineering, Nanyang Technological University, Singapore
`{xiazj0002, yhe, schan, cwfufu}@ntu.edu.sg`

^bDepartment of Mathematics, Rutgers University, USA
`fluo@math.rutgers.edu`

^cDepartment of Computer Science, Stony Brook University, USA
`gu@cs.sunysb.edu`

Abstract. Parameterizations have a wide range of applications in computer graphics, geometric design and many other fields of science and engineering. Although surface parameterizations have been widely studied and are well developed, little research exists on the volumetric data due to the intrinsic difficulties in extending surface parameterization algorithms to volumetric domain. In this paper, we present a technique for parameterizing star-shaped volumes using the Green’s functions. We first show that the Green’s function on the star shape has a unique critical point. Then we prove that the Green’s functions can induce a diffeomorphism between two star-shaped volumes. We develop algorithms to parameterize star shapes to simple domains such as balls and star-shaped polycubes, and also demonstrate the volume parameterization applications: volumetric morphing, anisotropic solid texture transfer and GPU-based volumetric computation.

1 Introduction

The recent decade has witnessed the great advancements of surface parameterizations, exemplified in a wide range of applications exhibited in science and engineering. Despite these successes, most real-world objects are in fact volumes rather than surfaces. It remains both unclear and challenging on how to generalize existing surface parameterization methods from surfaces to volumes. And with volume parameterization, we envision a large pool of applications that can benefit from the result, including solid texture mapping, volumetric tetrahedralization for simulation, and volumetric registration.

Due to the intrinsic difference between surfaces and volumes, many classical results on surface parameterization cannot be directly generalized to produce volume parameterization. For example, it is well-known that a harmonic map between a topological disk (a genus zero surface with a single boundary) and a planar convex domain is diffeomorphic (i.e., bijective and smooth), if the boundary map is homeomorphic (i.e., bijective and continuous). This result plays an important role in surface parameterization. Unfortunately, such an approach is not applicable to volumes, i.e., volumetric harmonic map is not guaranteed to be bijective even though the target domain is convex. In this paper, we aim at handling the challenges by proposing a theoretically sound algorithm that can produce a diffeomorphism between two star-shaped volumes.

Our volume parameterization method is strongly motivated by the property of electric field. Given a closed genus-0 metal surface S , let M denote its interior volume, i.e., $\partial M = S$. We construct an electric field by putting a positive electric charge at a point c inside M , and connecting the boundary surface S to the ground. The *electric potential* inside M is a *Green's function*, $G : M \rightarrow \mathbb{R}$, such that

$$\begin{cases} \Delta G(x) = \delta(x - c) \\ G|_{\partial M} \equiv 0, \end{cases} \quad (1)$$

where $\delta(x - c)$ is the Dirac function. In general, the level set of G , $G^{-1}(r), r \in \mathbb{R}^+$ or an isopotential surface is a smooth surface in M . The gradient of the electric potential ∇G is the *electric field*. *Electric field lines* are the integration curves of the electric field, i.e., the tangent vectors of the electric field lines are parallel to the electric field. Different electric field lines only intersect at the points where we put the electric charge, or at the critical point of the potential. Electric field lines start from the electric charge and are orthogonal to the iso-potential surfaces everywhere, in particular to the boundary surface ∂M .

If M is a star-shaped volume, every ray cast from c intersect S only once, and there are no other critical points of the potential. Therefore, all the iso-potential surfaces can be topological spheres and all electric field lines intersect only at point c (see Fig. 1). Since each point inside M is now uniquely determined by a corresponding electric field line and an iso-potential surface, determining the map between two star-shaped volumes is equivalent to constructing the map between the corresponding iso-potential surfaces and the electric field lines. Therefore, we map the boundary surface to the unit sphere, thereby putting each iso-potential surface to a concentric sphere, the electric field lines to the radii, and the center c to the origin. In this way, the star-shaped volume can be parameterized to the unit solid ball. With the help of ball parameterization, the map between two star shapes can then be constructed by mapping each shape to the unit ball and constructing a bijective map between the two unit balls. Such a constructed volumetric map is guaranteed to be a diffeomorphism.

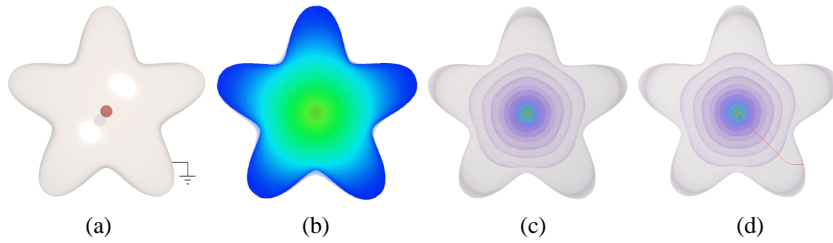


Fig. 1. Electric field on the star shape. Given a metal surface S , we put a positive charge at the center (the red point) and then connect S to the ground (shown in (a)). The electric field is a Green's function shown in (b). If the surface S is star-shaped, then the Green's function has a unique critical point. As a result, all iso-potential surfaces are topological spheres (shown in (c)). The electric field line (red curve in (d)) is perpendicular to all iso-potential surfaces.

Our contributions include

- First, we show that the Green’s function on star shapes has a unique critical point and all level sets inside the star shape are topological spheres. Then we prove that the Green’s function can induce a diffeomorphism between two star shapes. To our knowledge, this is the first constructive proof of the existence of a diffeomorphism between two non-trivial shapes.
- Secondly, based on our theoretical results, we develop algorithms to parameterize star shapes to star-shaped domains, such as solid balls and star-shaped polycubes.
- Thirdly, we showcase a variety of applications that benefit from our volume parameterization method, including volumetric morphing, anisotropic solid texture transfer and GPU-based volumetric computation.

The remaining of the paper is organized as follows. We first briefly discuss the previous work in Section 2. Next, we introduce the theoretic background in Section 3, and present our volume parameterization algorithm in Section 4. Experimental results are then reported in Section 5. We conclude this work in Section 6. The theoretic proofs are presented in the Appendix.

2 Previous Work

Extensive research has been done on surface parameterization due to its wide applications in computer graphics. The surveys of [1][2] provide excellent reviews on various kinds of mesh parameterization techniques. In the following, we briefly review the related work on volumetric meshing and volumetric harmonic map.

Labelle and Shewchuk introduced the isosurface stuffing algorithm to generate tetrahedron meshes with bounded dihedral angles in [3]. The volumetric discrete Laplace-Beltrami operator used in this work generalizes the *cotan* formula in the surface case; the *cotan* value of dihedral angles is used to replace those of corner angles. The range of the dihedral angles affects the parameterization quality. A Delaunay-based variational approach to isotropic tetrahedral meshing is introduced by Alliez et al. in [4]; this method can produce well-shaped tetrahedra by energy minimization. Tandem algorithm is introduced to isosurfaces extraction and simplification in [5]. The volumetric harmonic map depends on volumetric Laplacian; Zhou et al. [6] applied volumetric graph Laplacian to large mesh deformation.

Harmonicity in volumes can be similarly defined via the vanishing Laplacian, which governs the smoothness of the mapping function. Wang et al. [7] studied the formula of harmonic energy defined on tetrahedral meshes and computed the discrete volumetric harmonic maps by a variational procedure. Volumetric parameterization using fundamental solution method is introduced in [8] and applied to volumetric deformation and morphing. Other than that, harmonic volumetric parameterization for cylinder volumes is applied for constructing tri-variate spline fitting in [9]. All the above approaches rely on volumetric harmonic maps. Unfortunately, as pointed out previously in Section 1, these volumetric harmonic maps cannot guarantee bijective mappings even though the target domain is convex.

Besides the volumetric harmonic map, another stream of research studies the mean value coordinates for closed triangular mesh [10, 11]. Mean value coordinates are a powerful and flexible tool to define a map between two volumes. However, there is no guarantee that the computed map is a diffeomorphism.

Our approach differs intrinsically from these existing approaches in two-fold. First, we solve the Green's functions on star shapes and show that the resultant functions have unique critical points. As a result, the Green's function induced map is guaranteed to be a diffeomorphism. Second, we use fundamental solution method [12, 8, 13] rather than the conventional volumetric harmonic map [7], since the fundamental solution method is truly meshless, thus, it does not depend on the tetrahedral mesh. In sharp contrast, volumetric harmonic map heavily depends on the quality of the tetrahedral mesh. Irregular tetrahedralization may lead to numerical error and degeneracy of the volumetric harmonic map even on convex or star shapes.

Our work is also related to polycube map which can be used as the parametric domain for the volume parameterization. Tarini et al. pioneered a method to construct polycube map by projecting the vertices to the polycube domain [14]. Wang et al. presented an intrinsic approach to construct polycube map that is guaranteed to be a diffeomorphism [15]. Later, they developed a method that allows the users to freely specify the extraordinary points on the 3D models [16]. Lin et al. presented an automatic algorithm to construct polycube map with simple geometry and topology [17]. Using the divide-and-conquer strategy, He et al. developed a polycube map construction method that can process large 3D models [18].

3 Theoretic Foundation

This section briefly introduces the theoretic foundation of star shape parameterization; see the detailed proof in the Appendix section.

A volume M is called a *star shape* if there exists a point $\mathbf{c} \in M$ such that any ray cast from \mathbf{c} intersects the boundary of M only once. The point \mathbf{c} is called the center of M . In particular, any convex volume is a star shape, where any interior point can serve as the center. From the implementation point of view, computing the intersection of a ray with a surface is typically computationally expensive. Thus, we use an alternative approach to define a star shape:

Lemma 1. *A volume M is a star shape if and only if there exists a point $\mathbf{c} \in M$ such that for any boundary point $\mathbf{p} \in \partial M$,*

$$(\mathbf{c} - \mathbf{p}, \mathbf{n}(\mathbf{p})) \leq 0, \quad (2)$$

where $\mathbf{n}(\mathbf{p})$ is the normal vector at \mathbf{p} and (\cdot, \cdot) is the dot product.

The following lemmas reveal some nice properties of star shapes and lay a crucial role in our work.

Lemma 2 (Green's function on a star shape). *Suppose M is a star shape with a center $\mathbf{c} \in M$, G is the Green's function (see Eqn. (1)) with a pole at \mathbf{c} , then \mathbf{c} is the only critical point of G .*

Lemma 3. Suppose M is a star shape with a center $\mathbf{c} \in M$, G is the Green's function with a pole at \mathbf{c} . Then for any $r \in \mathbb{R}^+$, the level set $G^{-1}(r)$ is topologically equivalent to a sphere.

Let γ_1 and γ_2 be two integration curves of the gradient field, ∇G . If γ_1 and γ_2 intersect at point \mathbf{p} , i.e., $\mathbf{p} \in \gamma_1 \cap \gamma_2$, then $\nabla G(\mathbf{p})$ must be zero. Namely, \mathbf{p} must be a critical point of G . Since G has only one critical point \mathbf{c} , γ_1 and γ_2 only intersect at the center \mathbf{c} . Furthermore, each integration curve of ∇G intersects the boundary surface ∂M perpendicularly.

A map between two star-shaped volumes M and \tilde{M} with centers \mathbf{c} and $\tilde{\mathbf{c}}$, respectively, can be constructed in the following manner. First we compute a bijective map between their boundaries $\phi : \partial M \rightarrow \partial \tilde{M}$. Then we compute two Green's functions G and \tilde{G} on M and \tilde{M} with poles \mathbf{c} and $\tilde{\mathbf{c}}$, respectively. Let $r \in \mathbb{R}^+$, then the level set $G^{-1}(r) \subset M$ matches the level set $\tilde{G}^{-1}(r) \subset \tilde{M}$. Let $\mathbf{p} \in \partial M$, the integration curve through \mathbf{p} in M matches the integration curve through $\phi(\mathbf{p})$ in \tilde{M} . The centers of M and \tilde{M} are mapped to each other. Each interior point (other than the origin) is the intersection of a unique level set and a unique integration curve, therefore, every point in M can be uniquely mapped to a point in \tilde{M} .

Therefore, we arrive at the following theorem, which lays down the theoretic foundation of our volumetric parameterization algorithm.

Theorem 1. Suppose M and \tilde{M} are star-shaped volumes with centers \mathbf{c} and $\tilde{\mathbf{c}}$, G and \tilde{G} are Green's functions with poles at \mathbf{c} and $\tilde{\mathbf{c}}$, respectively. If the boundary map $\partial M \rightarrow \partial \tilde{M}$ is a diffeomorphism, then the map $f : M \rightarrow \tilde{M}$ induced by G and \tilde{G} is also a diffeomorphism.

Theorem 1 laid down the foundation of the proposed volume parameterization framework. We should point out that even though \mathbf{c} and $\tilde{\mathbf{c}}$ are poles of the Green's functions G and \tilde{G} , the induced map $f : M \rightarrow \tilde{M}$ is smooth everywhere including the pole \mathbf{c} since we define $f(\mathbf{c}) := \tilde{\mathbf{c}}$. This can be elucidated by the physical meaning of Green's function. Consider the phenomenon of a grounded conducting surface surrounding a charged body at the center \mathbf{c} . The electric potential inside the volume bounded by the surface is the Green's function. If the volume is a solid ball and the center is the origin, then parameterization induced by the Green function is equivalent to the polar coordinate. The center is the pole of the polar parameterization, but the mapping between two balls induced by the polar coordinates has no singularity [19].

Remark. Gergen showed that the gradient of a Green's function in a star-shaped three dimensional region never vanish[20]. This implies that there is no interior singularity of the Green function, therefore the level sets are topological spheres, the integration curves of the gradient field do not intersect either. This gives alternative proof for our main theoretic result.

4 Volume Parameterization Using Green's Functions

This section presents the algorithmic detail of parameterizing star-shaped volumes to simple domains, such as the unit ball and star-shaped polycubes.

4.1 Parameterizing a star shape to a ball

```

Input:  $S$ , the boundary mesh of a star-shaped volume  $M$ 
Output:  $f : M \rightarrow \mathbb{B}^3$  is diffeomorphism
1.1 Find the center of  $M$ ;
1.2 Compute the Green's function on  $M$ ,  $G_M : M \rightarrow \mathbb{R}$ ;
1.3 Map the center  $\mathbf{c}$  to the center of  $\mathbb{B}^3$ ,  $f(\mathbf{c}) = \mathbf{0}$ ;
1.4 Parameterize the boundary points by constructing a conformal spherical mapping  $\phi : \partial M \rightarrow \partial \mathbb{B}^3$ ;
1.5 for every interior vertex  $\mathbf{p} \in M$ 
1.6   Trace the integration curve  $\gamma$  from  $\mathbf{p}$  to the boundary point  $\mathbf{q} \in \partial M$ ;
1.7   Set  $f(\mathbf{p}) = \frac{\phi(\mathbf{q})}{G_M(\mathbf{p})+1}$ 
1.8 end for

```

Algorithm 1: Ball parameterization of star shapes.

Step 1. Star shape verification and center detection. The input of our algorithm is a closed genus-0 surface S which encloses a volume M , i.e., $S = \partial M$. S is represented by a triangular mesh with vertices $\{\mathbf{v}_i\}_{i=1}^n$. First, we need to verify whether M is star-shaped. If it is true, we determine the center of M . Note that for a given star shape, there could be infinite possible choices for the centers and the distribution of Green's function. A badly chosen center may introduce severe bias in the volume parameterization. Thus, we prefer a geometry-aware center, where a natural choice is a center that is close to the center of mass of M . This leads to the following linear constrained quadratic programming problem:

$$\begin{aligned} \min_{\mathbf{c}} \quad & \frac{1}{n} \sum_{i=1}^n \|\mathbf{c} - \mathbf{v}_i\|^2 \\ \text{subject to} \quad & (\mathbf{c} - \mathbf{v}_i, \mathbf{n}_i) \leq 0 \quad i = 1, \dots, n. \end{aligned}$$

The objective function aims to minimize the distance between the center \mathbf{c} and the center of mass, where the linear constraints precisely ensure the detected center \mathbf{c} satisfies the star shape requirement (see Eqn. 3). If M is not star-shaped, then no valid solution will be found. In our implementation, we use the MOSEK optimization software [21] to solve this quadratic programming problem.

Step 2. Computing Green's functions on M and \mathbb{B}^3 . Next, we compute the Green's function on the star-shaped volume M using the method detailed in the fundamental solution [12, 8]. Suppose we have an electric charge q_i at point \mathbf{p}_i , the electric potential caused by q_i at point \mathbf{r} is

$$K(q_i, \mathbf{p}_i; \mathbf{r}) = \frac{1}{4\pi} \frac{q_i}{|\mathbf{p}_i - \mathbf{r}|}.$$

We need to put m electric charges $\{q_i\}$ at m points $\{\mathbf{p}_i\}$ on an offset surface above the boundary surface of ∂M , such that on the boundary ∂M , the total potential equals zero,

$$G_M(\mathbf{r}) = \sum_{i=1}^m K(q_i, \mathbf{p}_i; \mathbf{r}) + G(1, \mathbf{c}; \mathbf{r}) = 0, \forall \mathbf{r} \in \partial M,$$

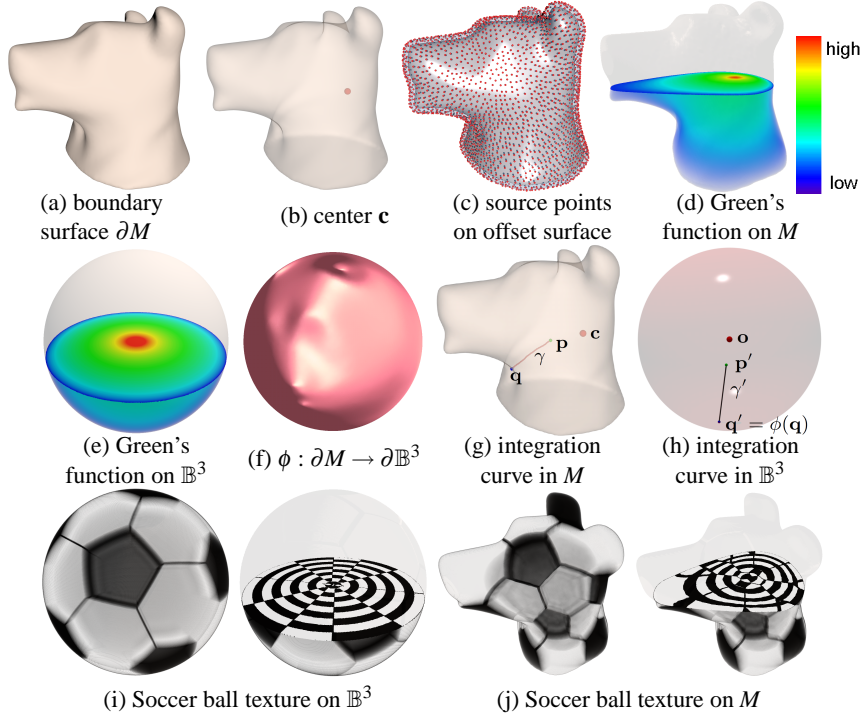


Fig. 2. Green's function induces a diffeomorphism between the star shape M and the unit ball B^3 . The input model is a triangular mesh (shown in (a)) which encloses a star-shaped volume. The red point in (b) shows the star shape center. Then we compute the Green's function on M using the fundamental solution method. (c) The source point placed on the offset surface of ∂M . (d) The Green's function on M . (e) The Green's function on B^3 which is given by a closed form formula $\frac{1}{r} - 1$. (f) The boundary parameterization by constructing a conformal spherical map $\phi : \partial M \rightarrow \partial B^3$. (g) We parameterize the interior point p by tracing the integration curve γ to the boundary point q . Note that the integration curve is perpendicular to the iso-surfaces of G . (h) The image of p is given by $\frac{\phi(p)}{G_M(p)+1}$. (i) and (j) show the volume rendering of a soccer ball texture on M and B^3 , respectively.

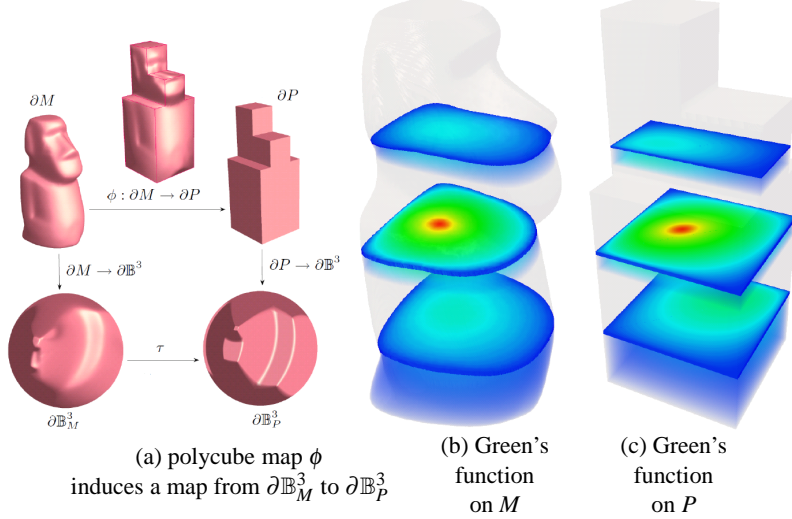


Fig. 3. Parameterizing a star shape M to a polycube P using the Green’s function. We first construct the conformal polycube map $\phi : \partial M \rightarrow \partial P$. Then, we parameterize M and P to the ball using Algorithm 1. The conformal polycube map ϕ induces an identity map between $\partial\mathbb{B}_M^3$ and $\partial\mathbb{B}_P^3$. The volume parameterization is then given by $f = f_M \circ f_P^{-1}$.

where q_i ’s are unknowns. The equation is converted to a dense linear system, which can be solved using the singular value decomposition method provided in Matlab. As suggested in [8], we place $m = 0.6n$ source points on the offset surface with offset distance equals 0.05 times the main diagonal of M .

The Green’s function on \mathbb{B}^3 (with the origin as the center) has a closed form, $G_B(p) = \frac{1}{r} - 1$, where r is the distance from p to the origin.

Step 3. Parameterizing the boundary points. Furthermore, we compute the boundary map $\phi : \partial M \rightarrow \mathbb{B}^3$. Since the boundary of the unit ball is the sphere \mathbb{S}^2 , the conformal spherical mapping [22] is a diffeomorphism, and thus, can serve as the boundary map.

Step 4. Parameterizing the interior points. The interior of the volume is represented by a tetrahedral mesh. We use Tetgen [23] to generate a tetrahedral mesh for a given surface mesh S to meet the boundary constraints. To improve the meshing quality, we employ the variational tetrahedral meshing technique [4] which can significantly reduce the slivers and produce well-shaped tetrahedral meshes. The tetrahedral mesh M is represented by $M = (V, E, F, T)$ where V, E, F , and T are the vertex, edge, face, and tetrahedra sets, respectively. The Green’s function G_M is represented as a piecewise linear function, $G_M : V \rightarrow \mathbb{R}$. The gradient of G can be computed as follows: suppose t_{ijkl} is a tetrahedron with vertices $\{v_i, v_j, v_k, v_l\}$, the face on the tetrahedron against vertex v_i is f_i ; similarly v_j, v_k , and v_l are against f_j, f_k , and f_l , respectively. We define \mathbf{s}_i to be the vector along the normal of f_i with length equal to 2 times the area of f_i , and so can $\mathbf{s}_j, \mathbf{s}_k, \mathbf{s}_l$ be defined. Then, the gradient of G_M in t_{ijkl} is a constant vector field

$$\nabla G_M = G_M(v_i)\mathbf{s}_i + G_M(v_j)\mathbf{s}_j + G_M(v_k)\mathbf{s}_k + G_M(v_l)\mathbf{s}_l.$$

We then define the vertex gradient as the average of the gradient vectors in the neighboring tetrahedra.

Finally, the parameterization from M to \mathbb{B}^3 , $f : M \rightarrow \mathbb{B}^3$ is constructed as follows. We map the center \mathbf{c} to the origin, i.e., the center of \mathbb{B}^3 . Given an interior point $\mathbf{p} \in M$ (other than the center \mathbf{c}), we trace the integration curve γ of the gradient field from \mathbf{p} , γ intersects the boundary surface ∂M at \mathbf{q} , then γ corresponds to the radius of \mathbb{B}^3 through the point $\phi(\mathbf{q})$. Suppose the Green's function value at \mathbf{p} is $G_M(\mathbf{p})$, then the image of \mathbf{p} is defined by

$$f(\mathbf{p}) = \frac{\phi(\mathbf{q})}{G_M(\mathbf{p}) + 1}.$$

Figure 2 illustrates the pipeline of parameterizing the dog head to a solid ball. To visualize the parameterization, we design a soccer ball texture on \mathbb{B}^3 and then map it to the dog head. Note that the iso-parameter surfaces in M are curved, but the cut view is obtained by a cutting plane. Thus, the texture on the intersection plane in Fig. 2(l) may look irregular.

Input: boundary meshes of a star shape M and a star-shaped polycube P

Output: $f : M \rightarrow P$ is diffeomorphism

- 2.1 Parameterize P to the unit ball $f_P : P \rightarrow \mathbb{B}_P^3$;
- 2.2 Parameterize M to the unit ball $f_M : M \rightarrow \mathbb{B}_M^3$;
- 2.3 Construct the polycube map $\phi : \partial M \rightarrow \partial P$;
- 2.4 Construct the map between two balls $\psi : \mathbb{B}_P^3 \rightarrow \mathbb{B}_M^3$ induced by the polycube map ϕ ;
- 2.5 Compute the composite map $f : M \rightarrow P$, $f = f_M \circ \psi \circ f_P^{-1}$.

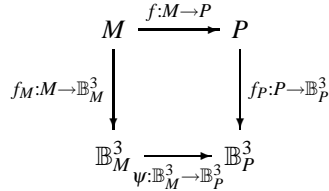
Algorithm 2: Polycube parameterization of star shapes

4.2 Parameterizing a star shape to a polycube

Ball parameterization is useful for the star shapes which resemble the geometry of the sphere. However, a general star shape may be significantly different from a ball. Thus, ball parameterization may result in large distortions. For such cases, we propose to use the star-shaped polycube as the parametric domain since it resembles the input object better than the ball.

Given a star shape M and a polycube P , we want to find a bijective and smooth map $f : M \rightarrow P$. Rather than computing the map directly, we first individually parameterize M and P to the unit balls using Algorithm 1 (see Sec 4.1). Then we seek a smooth map between two balls $\psi : \mathbb{B}_M^3 \rightarrow \mathbb{B}_P^3$. Finally, the polycube parameterization is given by the composite map $f = f_M \circ \psi \circ f_P^{-1}$.

The polycube parameterization can be illustrated clearly by the following commutative diagram:



Note that there exists infinitely many smooth maps between two unit balls, but different ψ could result in different volumetric parameterization. To find a low-distortion volumetric parameterization, i.e., mapping the head of Moai (see Fig. 3(a)) to the top of the polycube, and so on, the polycube map can serve as a feasible boundary constraint. In our implementation, we choose the approach of conformal polycube map (for genus-0 surfaces) [15]. Figure 3 illustrates the pipeline of parameterizing the star shapes to the polycube.

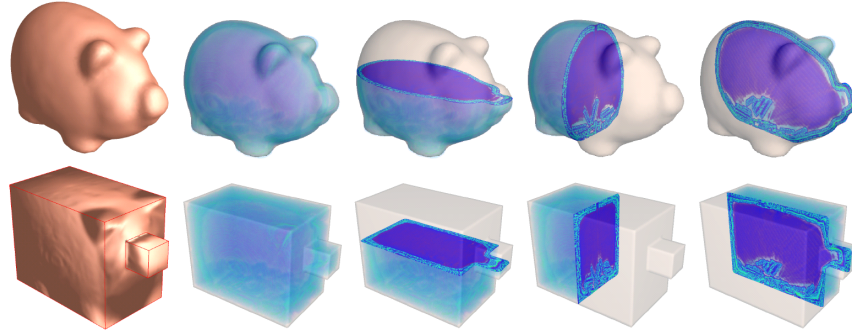


Fig. 4. Parameterizing the pig model to a polycube. Row 1 and 2 show the volume rendering of the volumetric data and polycube parameterization respectively.

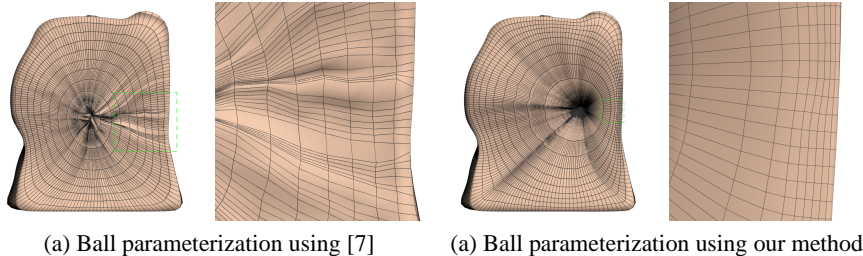


Fig. 5. Comparison. We map the dog head to unit ball using volumetric harmonic map [7] and our approach. As shown in the cut view of iso-parametric curves, our method is more robust and leads to hexahedral meshes with better quality. Our approach also guarantees that the iso-parametric curve which follow the direction of the gradient is orthogonal to the other two iso-parametric curves which span the iso-surface of the Green's function.

5 Experimental Results and Applications

This section showcases the experimental results and a variety of applications that can benefit from our star-shape parameterization method, from volumetric morphing to volume-based computation on the GPU.

Results. Figure 4 shows the parameterization of the pig-shaped coin box to a polycube. The volume rendering and the cut views reveal the quality of the parameterization.

We compared our method with the volumetric harmonic map method [7]. As mentioned above, the volumetric harmonic map is not guaranteed to be homeomorphic even though the domain is convex. In Figure 5, we parameterized the star model to the unit ball. As shown in the cut view and iso-parametric curves, our method is robust and leads to hexahedral meshes with better quality.

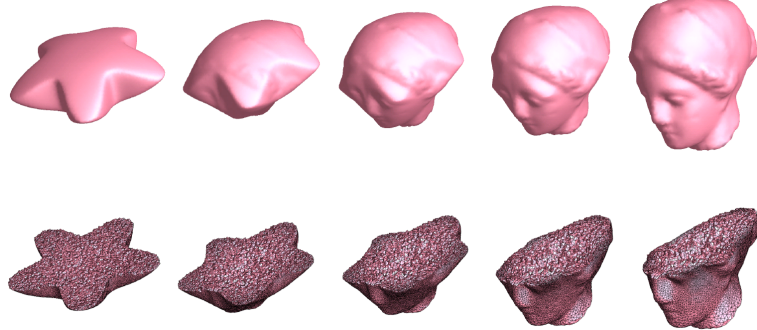


Fig. 6. Volumetric morphing between the star and the Venus head.

Volumetric Morphing. To morph from one star-shape to another, we parameterize them to a common parametric domain, such as a ball and then determine a smooth map (e.g., identity map in our current implementation) between the balls. Figure 6 shows a running example from star to Venus head.

Anisotropic Solid Texture. Solid textures [24], or anisotropic solid textures [25], allow us to fill the interior of 3D models with spatially-varying and anisotropic texture patterns. Takayama et al. [25] proposed a lapped texture approach [26] to synthesize anisotropic solid textures by pasting solid texture exemplars [24] repeatedly over the tetrahedron structure of 3D geometries. This approach can result in high-quality and large-scale solid textures with low computation cost; to create such a texture, the user, however, has to mark up volumetric tensor field and edit the texture in a geometry-dependent fashion.

Our star-shape volume parameterization method can further broaden the applicability of the lapped solid texture results to a larger pool of geometric models. As illustrated in Figure 7, we can first parameterize a given star shape that has been pre-synthesized with lapped solid texture to a solid ball using the Green’s function; hence, we can trans-

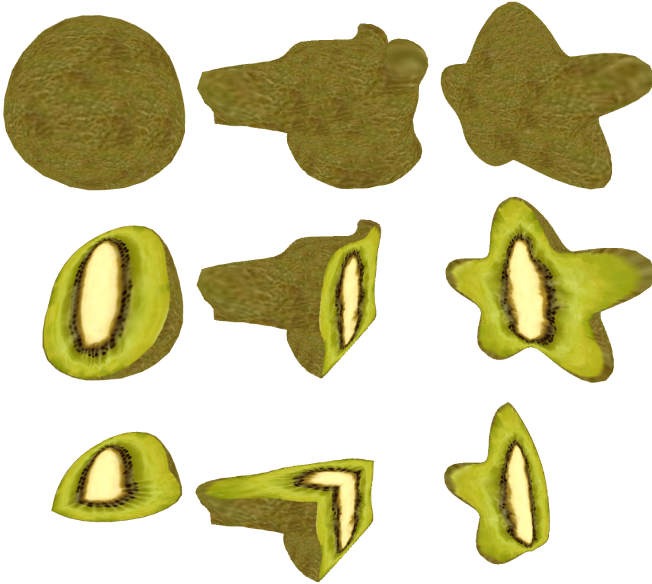


Fig. 7. Transferring the anisotropic solid texture from kiwi (column 1) to star shapes (column 2: dog head; column 3: star).

fer the synthesized texture information from the input geometric model to our star-shape model through the common parametric ground. Our approach allows the reuse of synthesized anisotropic solid textures without incurring additional texture synthesis. Furthermore, since our volume parameterization method is a diffeomorphism, we can guarantee the bijectivity and smoothness in the texture transfer process, as demonstrated in Figure 7.

GPU-based Volumetric Computation. Another advantage of having a smooth volume parameterization is the luxury of being able to perform computations throughout the volume by taking the computation process to the highly-structured parametric domain. Here we can parameterize the given star-shape model by a cube model (or polycube) so that the data inside the parametric domain can naturally be modeled by a 3D texture; as a result, we can carry out the computation on the GPU and further accelerate the computation performance.

In detail, we first parameterize a given star-shape model by a cube shape so that the reaction-diffusion data (concentration values, etc.) can be naturally modeled as 3D textures stored in our GPU implementation. Here, we employ and extend Turing’s reaction-diffusion model [27, 28] to three-dimensional, and expectedly, 3D sphere-like spot patterns will be developed when the chemical concentrations reach a dynamic equilibrium state. Furthermore, we employ Witkin and Kass’s method [29] to account for the distortion caused by the parameterization (since we compute the reaction-diffusion on the parameterization grid): Given the parameterization from star-shape to cube, we

compute the local Jacobian per voxel element over the 3D parameterization grid; then, we can compute the metric tensor as a three-by-three matrix $M = J^T J$. Hence, we can adaptively and locally modify the rate of diffusion by the diagonal values in the metric matrix; this allows us to temper the reaction-diffusion pattern, thereby compensating the volumetric distortion in the parameterization. Figure 8 shows the reaction-diffusion results on the Venus head model.

6 Conclusion and Future Work

This paper presented a volume parameterization technique for star shapes. On the theoretical side, we showed that the Green's function in a star-shaped volume has a unique critical point and then give a constructive proof of the existence of a diffeomorphism between two star shapes. On the application side, we developed algorithms to parameterize star shapes to simple domains such as solid balls and star-shaped polycubes. We also applied the star shape parameterization to several applications, such as volumetric morphing, anisotropic solid texture transfer and GPU-based volumetric computing.

The proposed technique has several limitations that can lead to further investigations. First, the current framework only applies to star-shaped volumes. However, most real-world shapes are not star-shaped. One possible solution to parameterize volumes of arbitrary topology and geometry is to segment the shape into a set of disjoint star shapes, then parameterize each shape individually, and finally glue patches together with a certain order of continuity. As a future direction, we will develop automatic techniques to facilitate the segmentation and gluing procedures. Second, from the implementation point of view, we solve the Green's function using fundamental solution method, which requires solving a dense linear system. Thus, it is not efficient when the number of source points is too large.

Acknowledgements

This work was partially supported by AcRF RG69/07, AcRF RG13/08, NSF CCF-1081424, ONR N000140910228, CCF-0448399, and CCF-0830550. We would like to thank Kenshi Takayama for the anisotropic solid textures and the anonymous reviewers for their constructive comments. Special thanks go to one reviewer who pointed out the reference [20].

References

1. Floater, M.S., Hormann, K.: Surface parameterization: a tutorial and survey. In: Advances in Multiresolution for Geometric Modelling. Springer (2005) 157–186
2. Sheffer, A., Praun, E., Rose, K.: Mesh parameterization methods and their applications. Foundations and Trends® in Computer Graphics and Vision **2**(2) (2006)
3. Labelle, F., Shewchuk, J.R.: Isosurface stuffing: fast tetrahedral meshes with good dihedral angles. ACM Trans. Graph. **26**(3) (2007) 57
4. Alliez, P., Cohen-Steiner, D., Yvinec, M., Desbrun, M.: Variational tetrahedral meshing. ACM Trans. Graph. **24**(3) (2005) 617–625

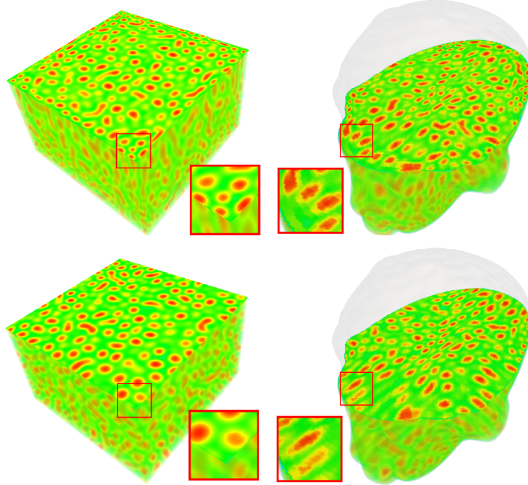


Fig. 8. Volumetric reaction-diffusion computation on the GPU. The first column shows the reaction-diffusion results in equilibrium state over the cube-based parametric domain, whereas the second column shows the reaction-diffusion results after mapped to the star-shaped model. Without distortion compensation by the metric matrix, we can see distortion in the lower right pattern, but such a distortion can be corrected (see upper row) if we take the metric matrix into account.

5. Attali, D., Cohen-Steiner, D., Edelsbrunner, H.: Extraction and simplification of iso-surfaces in tandem. In: Symposium on Geometry Processing. (2005) 139–148
6. Zhou, K., Huang, J., Snyder, J., Liu, X., Bao, H., Guo, B., Shum, H.Y.: Large mesh deformation using the volumetric graph laplacian. ACM Trans. Graph. **24**(3) (2005) 496–503
7. Wang, Y., Gu, X., Thompson, P.M., Yau, S.T.: 3d harmonic mapping and tetrahedral meshing of brain imaging data. In: MICCAI. (2004)
8. Li, X., Guo, X., Wang, H., He, Y., Gu, X., Qin, H.: Harmonic volumetric mapping for solid modeling applications. In: SPM. (2007) 109–120
9. Martin, T., Cohen, E., Kirby, M.: Volumetric parameterization and trivariate b-spline fitting using harmonic functions. In: Proceeding of Symposium on Solid and Physical Modeling. (2008)
10. Ju, T., Schaefer, S., Warren, J.D.: Mean value coordinates for closed triangular meshes. ACM Trans. Graph. **24**(3) (2005) 561–566
11. Floater, M.S., K  s, G., Reimers, M.: Mean value coordinates in 3d. Computer Aided Geometric Design **22**(7) (2005) 623–631
12. Fairweather, G., Karageorghis, A.: The method of fundamental solution for elliptic boundary value problems. Advances in Computational Mathematics **9**(1-2) (1998) 69–95
13. Li, X., Guo, X., Wang, H., He, Y., Gu, X., Qin, H.: Meshless harmonic volumetric mapping using fundamental solution methods. IEEE Transactions on Automation Science and Engineering **6**(3) (2009) 409–422
14. Tarini, M., Hormann, K., Cignoni, P., Montani, C.: Polycube-maps. ACM Trans. Graph. **23**(3) (2004) 853–860
15. Wang, H., He, Y., Li, X., Gu, X., Qin, H.: Polycube splines. Computer-Aided Design **40**(6) (2008) 721–733

16. Wang, H., Jin, M., He, Y., Gu, X., Qin, H.: User-controllable polycube map for manifold spline construction. In: ACM Symposium on Solid and Physical Modeling (SPM '08). (2008) 397–404
17. Lin, J., Jin, X., Fan, Z., Wang, C.C.L.: Automatic polycube-maps. In: GMP. (2008) 3–16
18. He, Y., Wang, H., Fu, C.W., Qin, H.: A divide-and-conquer approach for automatic polycube map construction. Comput. Graph. **33**(3) (2009) 369–380
19. Weber, H.J., Arfken, G.B.: Mathematical Methods For Physicists. Academic Press (2005)
20. Gergen, J.J.: Note on the green function of a star-shaped three dimensional region. American Journal of Mathematics **53**(4) (1931) 746–752
21. MOSEK: <http://www.mosek.com/>
22. Gu, X., Wang, Y., Chan, T.F., Thompson, P.M., Yau, S.T.: Genus zero surface conformal mapping and its application to brain surface mapping. TMI **23**(8) (2004) 949–958
23. Si, H.: Tetgen: A quality tetrahedral mesh generator and three-dimensional delaunay triangulator. <http://tetgen.berlios.de/>
24. Kopf, J., Fu, C.W., Cohen-Or, D., Deussen, O., Lischinski, D., Wong, T.T.: Solid texture synthesis from 2d exemplars. ACM Transactions on Graphics (Proceedings of SIGGRAPH 2007) **26**(3) (2007) 2:1–2:9
25. Takayama, K., Okabe, M., Ijiri, T., Igarashi, T.: Lapped solid textures: filling a model with anisotropic textures. ACM Trans. Graph. **27**(3) (2008) 1–9
26. Praun, E., Finkelstein, A., Hoppe, H.: Lapped textures. In: SIGGRAPH. (2000) 465–470
27. Turing, A.: The chemical basis of morphogenesis. Royal Society of London Philosophical Transactions Series B **237** (1952) 37–72
28. Turk, G.: Generating textures on arbitrary surfaces using reaction-diffusion. In: SIGGRAPH. (1991) 289–298
29. Witkin, A.P., Kass, M.: Reaction-diffusion textures. In: SIGGRAPH. (1991) 299–308

Appendix

We prove the main theoretical results in this appendix.

Lemma 1 *A volume M is a star shape if and only if there exists a point $\mathbf{c} \in M$ such that for any boundary point $\mathbf{p} \in \partial M$,*

$$(\mathbf{c} - \mathbf{p}, \mathbf{n}(\mathbf{p})) \leq 0, \quad (3)$$

where $\mathbf{n}(\mathbf{p})$ is the normal vector at the point \mathbf{p} .

Proof Assume the boundary surface ∂M is represented by the zero level set of an implicit function $f : \mathbb{R}^3 \rightarrow \mathbb{R}$, i.e., $\partial M = f^{-1}(0)$ and the interior points $\mathbf{r} \in M$ satisfy $f(\mathbf{r}) < 0$.

(\Rightarrow necessary condition) If M is a star shape, for any boundary point $\mathbf{p} \in M$, the ray $\mathbf{p} - \mathbf{c}$ intersects ∂M only once and the intersection point is \mathbf{p} . Thus, for any $\varepsilon \in [0, 1]$, the point $\mathbf{q} = \mathbf{p} + \varepsilon\mathbf{c} - \mathbf{p} \in M$ is inside M . Then, for a small $\varepsilon > 0$,

$$f(\mathbf{q}) = f(\mathbf{p}) + \varepsilon \nabla f(\mathbf{p}) \cdot (\mathbf{c} - \mathbf{p}) + O(\varepsilon^2 \|\mathbf{c} - \mathbf{p}\|^2).$$

Note that $f(\mathbf{p}) = 0$ and $f(\mathbf{q}_\varepsilon) \leq 0$, thus, $\nabla f(\mathbf{p}) \cdot (\mathbf{q}_\varepsilon - \mathbf{p}) \leq 0$. Since $\nabla f(\mathbf{p})$ points to the normal direction $\mathbf{n}(\mathbf{p})$, and $\mathbf{c} - \mathbf{p}$ has the same direction as $\mathbf{q}_\varepsilon - \mathbf{p}$, then $(\mathbf{c} - \mathbf{p}, \mathbf{n}(\mathbf{p})) \leq 0$.

(\Leftarrow sufficient condition) Given a point $\mathbf{c} \in M$, for every boundary point \mathbf{p} , $(\mathbf{c} - \mathbf{p}, \mathbf{n}(\mathbf{p})) \leq 0$ holds. Assume M is not a star shape, then there exists a ray from \mathbf{c} which

intersects ∂M at least twice. Without loss of generality, say \mathbf{p}_1 and \mathbf{p}_2 are the first two intersection points and \mathbf{p}_1 is closer to \mathbf{c} . Consider a point $\mathbf{q} = \varepsilon(\mathbf{p}_1 - \mathbf{p}_2) + \mathbf{p}_2$ with $\varepsilon > 0$. Clearly, \mathbf{q} is on the segment $\mathbf{p}_1\mathbf{p}_2$ and out of M . Thus, $f(\mathbf{q}) > 0$. Using Taylor expansion,

$$f(\mathbf{q}) = f(\mathbf{p}_2) + \varepsilon \nabla f(\mathbf{p}_2) \cdot (\mathbf{p}_1 - \mathbf{p}_2) + O(\varepsilon^2 \|\mathbf{p}_1 - \mathbf{p}_2\|^2).$$

Note that $f(\mathbf{p}_2) = 0$ and $\nabla f(\mathbf{p}_2)$ points to the same direction as normal $\mathbf{n}(\mathbf{p}_2)$, $\mathbf{p}_1 - \mathbf{p}_2$ points to the same direction as $\mathbf{c} - \mathbf{p}_2$, thus, $\nabla f(\mathbf{p}_2) \cdot (\mathbf{p}_1 - \mathbf{p}_2) \leq 0$ and $f(\mathbf{q}) \leq 0$, contradiction! Q.E.D.

Lemma 2 [Green's function on a star shape] Suppose M is a star shape with a center $c \in M$, G is the Green's function with a pole at c , then c is the only critical point of G .

Proof Without loss of generality, we assume c is at the origin in \mathbb{R}^3 . Let $B(c, \varepsilon)$ be a small ball centered at c with radius ε . Consider the following function, the inner product of the point $p = (x_1, x_2, x_3)$ and the gradient of G at p ,

$$f(p) = (p, \nabla G) = x_1 \frac{\partial G}{\partial x_1} + x_2 \frac{\partial G}{\partial x_2} + x_3 \frac{\partial G}{\partial x_3}.$$

By direct computation, it is easy to verify that

$$\Delta f = \left(\sum_k \frac{\partial^2}{\partial x_k^2} \right) \left(\sum_i x_i \frac{\partial G}{\partial x_i} \right) = 0.$$

In details,

$$\frac{\partial^2}{\partial x_k^2} \left(\sum_i x_i \frac{\partial G}{\partial x_i} \right) = 2 \frac{\partial^2 G}{\partial x_k^2} + \sum_i x_i \frac{\partial^3 G}{\partial x_k^2 \partial x_i},$$

therefore

$$\left(\sum_k \frac{\partial^2}{\partial x_k^2} \right) \left(\sum_i x_i \frac{\partial G}{\partial x_i} \right) = 2 \Delta G + \sum_i x_i \Delta \frac{\partial G}{\partial x_i}.$$

Because G is harmonic, therefore, $\frac{\partial G}{\partial x_i}$ is also harmonic, and the above equation equals zero.

Therefore $f(p)$ is a harmonic function on $M/B(c, \varepsilon)$. According to the maximum principle of harmonic maps, f reaches its max and min values on the boundary surfaces ∂M and $\partial B(c, \varepsilon)$. Here by definition, and c is the pole of f , f is negative on $\partial B(c, \varepsilon)$. Because M is a star shape, on ∂M , $(\mathbf{n}, p) > 0$, where \mathbf{n} is the normal on p to ∂M . ∇G is orthogonal to ∂M and is on the opposite direction of \mathbf{n} . Therefore, f is always negative in the whole volume $M/B(c, \varepsilon)$, ∇G is non-zero in $M/B(c, \varepsilon)$. Since ε is arbitrary, ∇G is non-zero for all points in $M/\{c\}$. We conclude that G has no critical points in M except c . Q.E.D.

Lemma 3 Suppose M is a star shape with a center $c \in M$, G is the Green's function with a pole at c . Then for any $r \in \mathbb{R}^+$, the level set $G^{-1}(r)$ is a topological sphere.

Proof Let $r \in \mathbb{R}^+$, $G^{-1}(r)$ is the level set of G . $G^{-1}(0)$ is the boundary of M , ∂M , which is a topological sphere. By lemma 2, there is no critical points in $G^{-1}([0, r])$. According to Morse theory, $G^{-1}(r)$ and $G^{-1}(0)$ share the same topology. In fact, we can start from a point $p \in G^{-1}(r)$ and trace along the integration curve of the gradient of G and reach a unique point q on $G^{-1}(0)$, this gives us a diffeomorphism from $G^{-1}(r)$ to $G^{-1}(0)$. Q.E.D.

Theorem 1 Suppose M and \tilde{M} are star-shaped volumes with centers c and \tilde{c} , G and \tilde{G} are Green's functions with the poles at c and \tilde{c} respectively. The Green's functions induce foliations. If the boundary map $\partial M \rightarrow \partial \tilde{M}$ is a diffeomorphism, the map $M \rightarrow \tilde{M}$ constructed using the foliations is a diffeomorphism.

Proof We first introduce the concepts of *foliation* and *leaf*.

A dimension m foliation of an n -dimensional manifold M is a covering by charts U_i together with maps $\phi_i : U_i \rightarrow \mathbb{R}^n$, such that on the overlaps $U_i \cap U_j$, the transition functions $\phi_{ij} = \phi_j \circ \phi_i^{-1}$ take the form

$$\phi_{ij}(x, y) = (\phi_{ij}^1(x), \phi_{ij}^2(x, y))$$

where x denotes the first $n - m$ coordinates, y denotes the last m coordinates. In each chart U_i the $x = \text{const}$ stripes match up with the stripes on U_j . The stripes piece together from chart to chart to form maximal connected injectively immersed submanifolds called the *leaves*.

The we show the proof. Let F_1 be the foliation of M by topological spheres induced by the level sets of G , F_2 be the foliation of M induced by the gradient lines of G . We choose an open cover of $M/\{c\}$, $\{(U_\alpha, \phi_\alpha)\}$, U_α is the union for leaves in F_2 , $U_\alpha = \cup f, f \in F_2$, such that $\phi_\alpha : U_\alpha \rightarrow \mathbb{R}^3$, leaves in F_1 are mapped to the planes $z = \text{const}$, leaves in F_2 are mapped to lines $(x, y) = \text{const}$. $\{(U_\alpha, \phi_\alpha)\}$ is a differential atlas. Similarly, we can construct a differential atlas of $\tilde{M}/\{\tilde{c}\}$, $\{\tilde{U}_\beta, \tilde{\phi}_\beta\}$, the level sets and the integration lines are mapped to canonical planes orthogonal to the z -axis and lines parallel to the z -axis.

The restriction of the map $f : M \rightarrow \tilde{M}$ on the local coordinate system

$$f_{\alpha\beta} = \tilde{\phi}_\beta \circ f \circ \phi_\alpha^{-1} : \phi_\alpha(U_\alpha) \rightarrow \tilde{\phi}_\beta(\tilde{U}_\beta)$$

has the following form

$$f_{\alpha\beta}(x, y, z) = (g(x, y), z),$$

where $g(x, y)$ is determined by the restriction of f on the boundary, $f|_{\partial M} : \partial M \rightarrow \partial \tilde{M}$. The restriction is a diffeomorphism, therefore $g(x, y)$ is a diffeomorphism, and $f_{\alpha\beta}$ is a diffeomorphism. Because U_α and \tilde{U}_β is arbitrarily chosen, f itself is a diffeomorphism. Q.E.D.